DALTON

Homo- and hetero-dinuclear metal complexes of bridging ligands containing phenol and azole moieties. Structure, spectroscopy, electrochemistry and magnetochemistry †

Sujit K. Dutta,[a] Kausik K. Nanda,[a] Ulrich Flörke,[b] Mohan Bhadbhade[c] and Kamalaksha Nag*[,a]

[a] *Department of Inorganic Chemistry, Indian Association for the Cultivation of Science, Calcutta 700032, India*

[b] *Anorganische und Analytische Chemie, Universitat-Gesamthochschule Paderborn, D-33098 Paderborn, Germany*

[c] *Central Salt and Marine Chemicals Research Institute, Bhavnagar 364002, India*

A series of phenoxo-bridged homo- and hetero-dinuclear complexes of 4-methyl-2,6-bis(5-methylpyrazol-3-yl)-phenol (H_3L^1) have been synthesized and characterized. Variable-temperature magnetic susceptibility measurements carried out for the homo-dinuclear complexes $[Cu_2(H_2L^1)_2][ClO_4]_2$ **1**, $[Cu_2(H_2L^1)(acac)_2][ClO_4]$ **2**, $[Cu_2(H_2L^1)(\mu\text{-}OH)Cl_2]$ **3**, $[Ni_2(H_2L^1)_2(H_2O)_4][ClO_4]_2$ **4** and $[Fe_2(H_2L^1)_4(\mu\text{-}OH)_2]\cdot 4H_2O$ **7** have shown that in all the cases the dinuclear metal centres are antiferromagnetically coupled with the following values of the exchange coupling constant J: -242 (**1**), -55 (**2**), -170 (**3**), -24 (**4**) and -11 cm^{-1} (**7**). The ESR spectra of the heterodinuclear complexes $[ZnCu(H_2L^1)_2][ClO_4]_2\cdot 2H_2O$ **5** and $[ZnMn(H_2L^1)_2Cl_2]$ **6** have been examined. The ^{1}H NMR spectra of the dicopper(II) complexes **1** and **2** are reasonably sharp and the isotropic shifts of **1** are relatively less compared to those of **2**. The crystal structures of **7** and **2**·$CHCl_3$ have been determined. That of **7** comprises two edge-shared sterically non-equivalent FeO_4N_2 distorted octahedra. The structure of **2**·$CHCl_3$ consists of two nearly square-planar copper(II) centres supported by a phenoxide bridge. The cryomagnetic behaviour of two phenoxo-bridged dimeric iron(III) complexes derived from a bis(iminomethyl)triphenol and a bis(aminomethyl)triphenol have also been studied.

A topic of considerable interest to co-ordination chemists is the effect of electronic communication between metal centres mediated through mono- or poly-atomic bridges. Depending upon the nature of the bridge, intramolecular interaction can profoundly influence magnetic,[1,2] redox [3] and spectroscopic [4,5] properties of metal complexes, and also their chemical reactivities.[6] Functions of certain metalloproteins containing two or more metal centres in their active sites are known to be regulated by the bridging groups therein.[7] The importance of exchange coupling in metallobiomolecules and the quest for new magnetic materials have synergistically influenced the growth of activities on magnetostructural relationships. While the spin-exchange behaviour of dinuclear metal complexes is now better understood,[1,2,4,8,9] the focus of attention is shifting to more complicated polymetallic systems.[10]

Among variously bridged complexes, μ-phenolate complexes have been extensively studied.[11–18] Similarly, azolate-bridged complexes [19] have also received considerable attention. We considered that suitable juxtaposition of phenol and azole moieties in a compound will lead to the formation of multinuclear complexes. Thus 4-methyl-2,6-bis(5-methyl-pyrazol-3-yl)phenol H_3L^1 (Scheme 1) has been synthesized. Herein we report the chemistry of several homo- and hetero-dinuclear complexes of H_3L^1 and compare the magnetic properties of the diiron(III) complexes derived from H_3L^1, H_3L^2 and H_3L^3.

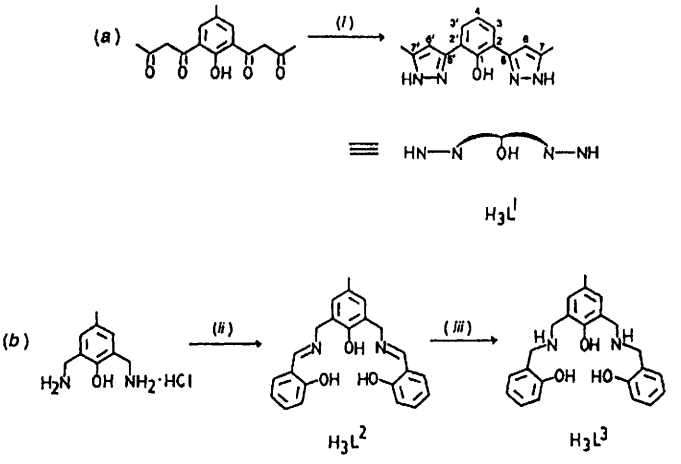

Scheme 1 (*i*) $N_2H_4\cdot H_2O$; (*ii*) NEt_3, $C_6H_4(OH)CHO$; (*iii*) $NaBH_4$

Experimental

Materials

All chemicals were obtained from commercial sources and used as received. Metal perchlorate salts were prepared from commercially available reagent-grade metal salts and perchloric acid.

Preparation of proligands

H_3L^1. 2,6-Diacetyl-4-methylphenol prepared by the method of Mandal and Nag [20] was first converted into the 2,6-bis(diketonyl)-4-methylphenol by slight modification of the procedure reported by Bailey *et al.* [21] This compound (2.8 g, 10 mmol) was dissolved in CH_2Cl_2 (100 cm^3) and treated with $N_2H_4\cdot H_2O$ (1 g, 20 mmol) in MeOH (10 cm^3). The solution was stirred at room temperature for 2 h and then refluxed for 0.5 h, during which time yellow crystals of H_3L^1 deposited. The product was filtered off after removing the bulk of the solvent on a rotary evaporator. However, it could not be recrystallized due to the lack of suitable solvents; yield 2.4 g (85%), m.p. 220 °C. NMR [$(CD_3)_2SO$]: ^{1}H, δ 2.26 (9 H, s, Me), 6.60 (2 H, s, pyrazolyl), 7.46 (2 H, s, aromatic), 11.7 (1 H, br, OH) and 12.8 (2 H, br, NH); ^{13}C, δ 20.3 (Me), 101.6 (7,7′-C), 102.9 (6,6′-C),

† *Non-SI units employed:* G = 10^{-4} T, $\mu_B \approx 9.27 \times 10^{-24}$ J T^{-1}.

117.4 (5,5′-C), 126.5 (4-C), 127.2 (3,3′-C), 139.3 (2,2′-C) and 150.3 (1-C).

H_3L^2. A methanol solution (100 cm^3) of 2,6-bis-(aminomethyl)-4-methylphenol monohydrochloride[22] (0.405 g, 2 mmol), triethylamine (0.2 g, 2 mmol) and salicylaldehyde (0.49 g, 4 mmol) was refluxed for 1 h and then filtered hot. The filtrate on rotary evaporation to *ca.* 30 cm^3 deposited yellow crystals, which were filtered off and recrystallized from boiling EtOH; yield 0.6 g (80%), m.p. 190 °C. ^1H NMR [$(CD_3)_2SO$]: δ 2.32 (3 H, s, Me), 4.0 (br, OH), 4.92 (4 H, s, CH_2), 6.7–7.7 (10 H, m, aromatic) and 8.78 (2 H, s, CH=N).

H_3L^3. A stirred MeOH solution (100 cm^3) of H_3L^2 (0.75 g, 2 m mol) was treated with small portions of an aqueous solution of $NaBH_4$ (*ca.* 2 mol dm^{-3}) till the yellow solution became colourless. A major part of the solvent was removed on a rotary evaporator, diluted with water (300 cm^3) and acidified with HCl (6 mol dm^{-3}) to pH *ca.* 2. The solution was then slowly treated with aqueous ammonia to pH ≈ 10 and extracted with $CHCl_3$ (2 × 50 cm^3). The $CHCl_3$ layer was dried over Na_2SO_4 and evaporated to dryness, and the white residue recrystallized from $CHCl_3$–MeOH (1:1); yield 0.5 g (66%), m.p. 204–205 °C. ^1H NMR ($CHCl_3$): δ 2.20 (3 H, s, Me), *ca.* 4.0 (br, NH and OH), 4.13 (8 H, s, CH_2) and 6.6–7.6 (10 H, m, aromatic).

Preparation of the complexes

$[Cu_2(H_2L^1)_2][ClO_4]_2$ 1. To a stirred suspension of H_3L^1 (0.54 g, 2 mmol) in MeOH (50 cm^3) were added NEt_3 (0.2 g, 2 mmol) and $Cu[ClO_4]_2·6H_2O$ (0.74 g, 2 mmol). In a few minutes a clear green solution was obtained, which on concentration afforded bright green crystals of complex **1**. The product was filtered off and recrystallized from MeOH (0.73 g, 85%).

$[Cu_2(H_2L^1)(acac)_2][ClO_4]$ 2. A mixture of complex **1** (0.86 g, 1 mmol) and copper(II) bis(acetylacetonate) (0.52 g, 2 mmol) was dissolved in MeOH (100 cm^3) and refluxed for 2 h. The colour changed from deep green to light green. Concentration to *ca.* 40 cm^3 on a rotary evaporator followed by standing overnight gave yellowish green crystals of **2** which were filtered off and recrystallized from MeOH (0.9 g, 65%).

$[Cu_2(H_2L^1)(\mu\text{-}OH)Cl_2]$ 3. A mixture of H_3L^1 (0.27 g, 1 mmol) and $CuCl_2·2H_2O$ (0.34 g, 2 mmol) in MeOH (100 cm^3) was stirred at room temperature for 2 h. During this period H_3L^1 dissolved and concomitantly complex **3** deposited as green microcrystals. The product was filtered off and recrystallized from dimethylformamide (0.34 g, 70%).

$[Ni_2(H_2L^1)_2(H_2O)_4][ClO_4]_2$ 4. This compound was prepared in the same way as **1** using $Ni[ClO_4]_2·6H_2O$ as the metal salt; sky blue crystals were obtained from MeOH, yield 75%.

$[ZnCu(H_2L^1)_2][ClO_4]_2·2H_2O$ 5. The mononuclear complex $[Cu(H_2L^1)_2]$ was generated *in situ* by refluxing a mixture of H_3L^1 (0.54 g, 2 mmol) and $Cu(acac)_2$ (0.26 g, 1 mmol) in MeOH (100 cm^3) for 0.5 h, when the product precipitated as a grey material. To this slurry was added $Zn[ClO_4]_2·6H_2O$ (0.38 g, 1 mmol) and the reflux continued for 0.5 h to obtain a clear green solution. The bulk of the solvent (*ca.* 80 cm^3) was removed on a rotary evaporator and the solution kept at 5 °C overnight. The product was filtered off and recrystallized from EtOH as brown crystals (0.5 g, 55%).

$[ZnMn(H_2L^1)_2Cl_2]$ 6. The dinuclear zinc(II) complex $[Zn_2(H_2L^1)_2][ClO_4]_2$ was first prepared by stirring a mixture of H_3L^1 (0.54 g, 2 mmol), NEt_3 (0.2 g, 2 mmol) and $Zn[ClO_4]_2·6H_2O$ (0.66 g, 2 mmol) in MeOH (60 cm^3) for 0.5 h. The clear light yellow solution thus obtained was purged with N_2 and then treated with solid $MnCl_2·4H_2O$ (0.4 g, 1 mmol). The solution was refluxed for 1 h under N_2 and then reduced to *ca.* 15 cm^3 by flash evaporation. Cooling at 5 °C afforded light greenish yellow crystals of complex **6**, which were filtered off and dried *in vacuo* (0.4 g, 60%).

$[Fe_2(H_2L^1)_4(\mu\text{-}OH)_2]·4H_2O$ 7. To a stirred suspension of H_3L^1 (0.54 g, 2 mmol) in MeOH (50 cm^3) was added solid $Fe[ClO_4]_3·6H_2O$ (0.46 g, 1 mmol). After a few minutes NaO_2CMe (0.74 g, 8 mmol) was added to the resulting deep violet solution, which changed to deep red. Stirring was continued for 2 h during which time complex **7** deposited as red microcrystals. Recrystallization was from MeOH–CH_2Cl_2 (1:2); yield 0.45 g (70%). An alternative method involves the use of NEt_3 (2 mmol) in the place of NaO_2CMe.

$[(FeL^2)_2]$ 8. A mixture of H_3L^2 (0.375 g, 1 mmol), NaO_2CMe (0.28 g, 6 mmol) and $Fe[ClO_4]_3·6H_2O$ (0.46 g, 1 mmol) in MeOH (60 cm^3) was stirred for 2 h. The red precipitate obtained was filtered off and recrystallized from MeCN (0.34 g, 80%).

$[(FeL^3)_2]·2H_2O$ 9. This compound was obtained (70%) in the same way as **8**.

The C, H and N analyses were performed on a Perkin-Elmer model 240C elemental analyser; nickel and copper were estimated gravimetrically and iron volumetrically after decomposition with mineral acids. The data are given in Table 1.

CAUTION: all the perchlorate salts reported here are potentially explosive and therefore should be handled with care.

Physical measurements

Infrared spectra were recorded on a Perkin-Elmer spectrophotometer using KBr discs, electronic spectra on a Shimadzu UV-160A spectrophotometer and ^1H and ^{13}C NMR spectra on a Bruker AC-250 spectrometer. For ^1H NMR spectra $SiMe_4$ was used as the reference (δ 0), while for the ^{13}C NMR spectrum the solvent $(CD_3)_2SO$ signal. X-Band ESR spectra of solutions at room temperature and 77 K were recorded on a Bruker 2000D spectrometer using diphenylpicrylhydrazyl (dpph, $g = 2.0037$) as the calibrant. Variable-temperature magnetic susceptibility data were obtained in the range 80–295 K by using a Faraday balance comprising a Bruker E1068 magnet, a Sartorius 4432 microbalance and a Bruker VT 1000 temperature controller. Susceptibility data were corrected for diamagnetism using Pascal constants. Cyclic voltammetric measurements were carried out with a Bioanalytical Systems BAS 100B electrochemical analyser. A three-electrode assembly (BAS) comprising a platinum working electrode, a platinum auxiliary electrode and a Ag–AgCl reference electrode was used. The reference electrode was separated from the bulk electrolyte by a salt bridge containing the supporting electrolyte tetraethylammonium perchlorate (0.1 mol dm^{-3}) in MeCN–water (1:1) with the help of a Vycor and heat-shrinkage tubing. In all the cases the potentials recorded were automatically compensated for *iR* drop in the cell. Under the experimental condition used the reversible oxidation of ferrocene (MeCN, Pt) occurred at 0.355 V.

Crystallography

Diffraction-quality crystals of complex **7** were obtained by diffusing MeOH into a CH_2Cl_2 solution of the compound. Intensity data were collected with an Enraf-Nonius CAD4 diffractometer at 293 K using graphite-monochromatized Cu-Kα radiation (μ/cm^{-1} 42.69). Pertinent crystallographic data are summarized in Table 3. Three standard reflections

monitored periodically showed the absence of either crystal decay or orientation loss. The intensity data were corrected for Lorentz-polarization effects and for absorption by an empirical method.[23] The structure was solved by direct methods using the program MULTAN 82.[24] Some of the hydrogen atoms were located in the Fourier difference map and the rest were generated using stereochemical constraints. The final cycles of full-matrix least-squares refinement were carried out in two blocks, each block containing an iron atom and the two ligand molecules with the bridging hydroxyl groups common to both blocks. The refinement on F converged to $R = 0.046$ and $R' = 0.025$ and the difference map at this stage showed ripples ranging between $+0.24$ and -0.30 e Å^{-3}.

Single crystals of complex **2**·$CHCl_3$ were obtained by diffusing Et_2O into a $CHCl_3$ solution of **2**. As the crystals spontaneously lose the solvent molecule on removal from the mother-liquor a suitable crystal along with the mother-liquor was sealed in a Lindemann capillary and mounted on a Siemens R3m diffractometer for intensity data collection at 297 K. Table 3 summarizes the relevant crystallographic data. A Lorentz-polarization correction was applied and semi-empirical absorption *via* ψ-scans. The structure was solved by direct methods using the program SHELXTL PLUS[25] and refined by full-matrix least squares on F^2 using the program SHELXL 93.[26] Scattering factors used for **2**·$CHCl_3$ and **7** were those given in ref. 27. During data collection considerable decay of the crystal of **2**·$CHCl_3$ occurred (36% loss of standard intensity). The position of the perchlorate anion was not fully resolved, only the chlorine and three oxygen atom sites with half occupation being determined. Diffuse electron-density peaks in the vicinity could not be assigned successfully to any other atom sites. The $CHCl_3$ solvent molecule is disordered over two different but neighbouring sites, each refined with an occupation factor of 0.5. Refinement of the cation was straightforward and converged easily. However, the overall structure refinement was poor [$R = 0.148$, $wR_2 = 0.531$ (on all data)] and hence the crystallographic results will not be reported in detail.

Complete atomic coordinates, thermal parameters and bond lengths and angles have been deposited at the Cambridge Crystallographic Data Centre. See Instructions for Authors, *J. Chem. Soc., Dalton Trans.*, 1996, Issue 1.

Results and Discussion

Synthesis

Although compound H_3L^1 has three dissociable protons, only the phenol is deprotonated upon reaction with the perchlorate salts of copper(II), nickel(II), zinc(II) and iron(III) in the presence of triethylamine. The homodinuclear complexes $[Cu_2(H_2L^1)_2][ClO_4]_2$ **1**, $[Ni_2(H_2L^1)_2(H_2O)_4][ClO_4]_2$ **4**, $[Zn_2(H_2L^1)_2][ClO_4]_2$ and $[Fe_2(H_2L^1)_4(\mu\text{-}OH)_2]\cdot 4H_2O$ **7** have been prepared in this way. As will be seen from the crystal structure of **7**, unlike in **1** and **4** the phenolate oxygens do not act as bridges between the two iron(III) centres. Attempts to prepare a μ-carboxylato-di-μ-phenolato-diiron(III) core were not successful. In contrast to the formation of complex **1**, when 2 equivalents of copper(II) chloride are treated with 1 equivalent of H_3L^1 the hydroxo-bridged dicopper(II) complex $[Cu_2(H_2L^1)(\mu\text{-}OH)Cl_2]$ **3** is obtained. The dicopper(II) heterochelate $[Cu_2(H_2L^1)(acac)_2][ClO_4]$ **2** has been synthesized by equilibrating a mixture of 1 equivalent of complex **1** and 2 equivalents of $Cu(acac)_2$. The ease with which **2** has been isolated indicates that reaction (1) is shifted far to the right due

$$[Cu_2(H_2L^1)_2]^{2+} + 2Cu(acac)_2 \rightleftharpoons 2[Cu_2(H_2L^1)(acac)_2]^{+} \quad (1)$$

to the greater overall stability constant of the product compared to those of the reactants.

The heterodinuclear complexes $[ZnCu(H_2L^1)_2][ClO_4]_2\cdot 2H_2O$ **5** and $[ZnMn(H_2L^1)_2Cl_2]$ **6** have been prepared by adopting two different approaches. It is convenient to obtain **5** by treating zinc(II) perchlorate with the mononuclear copper(II) complex $[Cu(H_2L^1)_2]$, while replacement of one of the zinc atoms of $[Zn_2(H_2L^1)_2][ClO_4]_2$ with $MnCl_2\cdot 4H_2O$ readily affords **6**.

Both H_3L^2 and H_3L^3 are potentially pentadentate ligands with three phenolic residues. However, they readily form the dimeric iron(III) complexes $[(FeL^2)_2]$ **8** and $[(FeL^3)_2]\cdot 2H_2O$ **9** when treated with iron(III) perchlorate in the presence of sodium acetate. As will be seen later, the dimeric compositions of these neutral compounds are consistent with their magnetic properties.

Characterization

The IR spectra of all the complexes derived from H_3L^1 exhibit two characteristic bands due to the ligand [δ(NH) and ν(C=N) at about 1620–1600 and 1575–1565 cm^{-1}]. In the case of $[Cu_2(H_2L^1)(\mu\text{-}OH)Cl_2]$ **3** a sharp band observed at 3270 cm^{-1} can be attributed to the presence of the bridging hydroxo moiety, while for $[Fe_2(H_2L^1)_4(\mu\text{-}OH)_2]\cdot 4H_2O$ **7** this band is shifted to a higher energy, 3350 cm^{-1}. By contrast to the hydroxo species, the ν(OH) due to bound/or lattice water molecules occurs as a broad feature in the range 3400–3500 cm^{-1}. Complex **3** additionally displays a band at 310 cm^{-1}, which is absent either for H_3L^1 or the other complexes, and is considered to be due to ν(Cu–Cl). The presence of the acetylacetonate moieties in **2** is inferred from the C···C and C···O stretchings at 1580 and 1520 cm^{-1}, respectively. The complex $[(FeL^2)_2]$ **8** is characterized by a band at 1630 cm^{-1} due to ν(C=N), while the diagnostic features of $[(FeL^3)_2]\cdot 2H_2O$ **9** are a band and a shoulder at 3220 and 1610 cm^{-1} due to ν(NH) and δ(NH), respectively.

The UV/VIS spectral data of the complexes are given in Table 2. In the visible region a single absorption band is observed for each of the copper(II) complexes $[Cu_2(H_2L^1)(acac)_2][ClO_4]$ **2**, $[Cu_2(H_2L^1)(\mu\text{-}OH)Cl_2]$ **3** and $[ZnCu(H_2L^1)_2][ClO_4]_2\cdot 2H_2O$ **5** at 610, 700 and 630 nm, respectively. By contrast, two peaks are observed at 760 and 600 nm for $[Cu_2(H_2L^1)_2][ClO_4]_2$ **1**. All these complexes show a strong band between 335 and 325 nm which can be assigned to ligand-to-metal charge transfer (l.m.c.t.).

The visible spectrum of the dinickel(II) complex **4** has features typical of octahedral nickel(II) complexes with $^3A_{2g} \longrightarrow {}^3T_{2g}$ and $^3A_{2g} \longrightarrow {}^3T_{1g}(F)$ transitions occurring at 1200 and 590 nm, respectively. A third band at 350 nm is most likely due to a $^3A_{2g} \longrightarrow {}^3T_{1g}(P)$ transition admixed with l.m.c.t.

A lone $PhO^- \rightarrow Fe^{III}$ charge transfer band is exhibited in the visible region of the spectrum by all the three diiron(III) complexes **7**–**9**. However, this band is significantly more intense for **7** ($\lambda_{max} = 510$ nm, $\varepsilon = 8100$ dm^3 mol^{-1} cm^{-1}) than for **8**

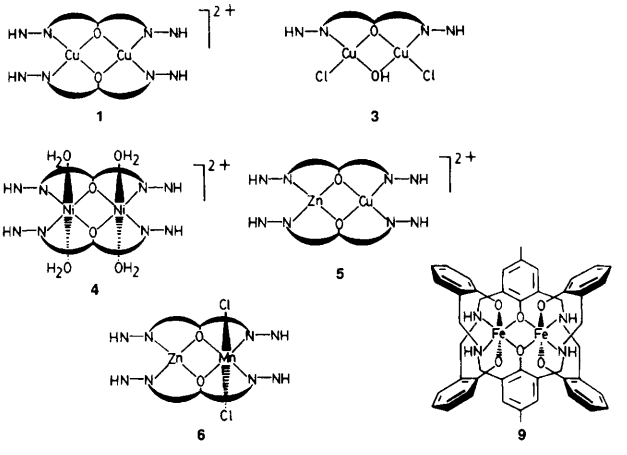

Table 1 Analytical data for the proligands and metal complexes

Compound	Analysis (%)* C	H	N	M
H_3L^1	67.4 (67.15)	6.05 (5.95)	20.95 (21.1)	
H_3L^2	74.1 (73.8)	5.8 (5.9)	7.45 (7.5)	
H_3L^3	73.2 (73.0)	6.8 (6.9)	7.45 (7.4)	
1 $[Cu_2(H_2L^1)_2][ClO_4]_2$	42.1 (41.85)	3.55 (3.5)	13.15 (13.0)	14.65 (14.8)
2 $[Cu_2(H_2L^1)(acac)_2][ClO_4]$	43.7 (43.4)	4.15 (4.2)	7.95 (8.1)	18.1 (18.35)
3 $[Cu_2(H_2L^1)(\mu\text{-}OH)Cl_2]$	37.6 (37.5)	3.25 (3.3)	11.4 (11.6)	26.1 (26.35)
4 $[Ni_2(H_2L^1)_2(H_2O)_4][ClO_4]_2$	39.4 (39.0)	4.0 (4.1)	12.25 (12.15)	12.5 (12.7)
5 $[ZnCu(H_2L^1)_2][ClO_4]_2\cdot 2H_2O$	39.8 (40.1)	3.65 (3.8)	12.2 (12.45)	
6 $[ZnMn(H_2L^1)_2Cl_2]$	50.15 (49.65)	4.3 (4.4)	15.6 (15.45)	
7 $[Fe_2(H_2L^1)_4(\mu\text{-}OH)_2]\cdot 4H_2O$	56.3 (56.0)	5.25 (5.45)	17.5 (17.4)	8.5 (8.7)
8 $[(FeL^2)_2]$	64.5 (64.65)	4.35 (4.45)	6.45 (6.55)	12.95 (13.1)
9 $[(FeL^3)_2]\cdot 2H_2O$	61.65 (61.45)	5.5 (5.55)	6.3 (6.25)	12.6 (12.45)

* Calculated values are given in parentheses.

Table 2 Electronic spectral data for the complexes

Complex	λ_{max}/nm (ε/dm^3 mol^{-1} cm^{-1})
1[a]	760 (260), 600 (340), 330 (9500)
2[a]	610 (150), 325 (8100)
3[b]	700 (240), 335 (6300)
4[a]	1200 (24), 590 (22), 350 (7100)
5[c]	630 (120), 335 (7500)
6[c]	390 (sh), 320 (12 400)
7[b]	510 (8100), 350 (sh) (35 000), 335 (47 000)
8[b]	470 (2150), 315 (sh) (6600)
9[b]	480 (2300), 315 (sh) (4000)

[a] In MeCN. [b] In dimethylformamide. [c] In MeOH.

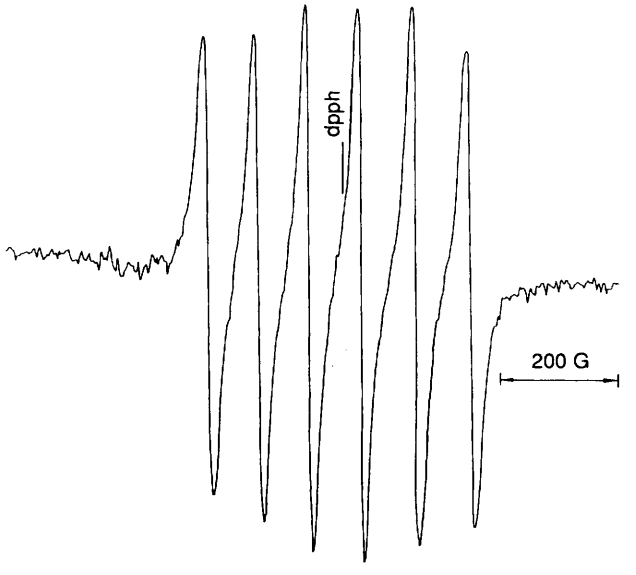

Fig. 1 The ESR spectrum of $[ZnMn(H_2L^1)Cl_2]$ **6** in dimethylformamide solution at room temperature. Microwave frequency 9.72 GHz

(470 nm, 2150 dm^3 mol^{-1} cm^{-1}) and **9** (480 nm, 2300 dm^3 mol^{-1} cm^{-1}).

The ESR spectrum of $[ZnCu(H_2L^1)_2][ClO_4]_2\cdot 2H_2O$ **5** in MeCN solution at room temperature has the expected four-line features of a copper(II) ion ($I = \frac{3}{2}$) with $g_{iso} = 2.112$ and $A_{iso} = 78$ G. In frozen solution the spectrum shows axial symmetry with $g_\perp < g_\parallel$, indicating a $d_{x^2-y^2}$ ground state for the metal ion, typical of square-planar or square-pyramidal copper(II) complexes. The spin-Hamiltonian parameters are estimated to be $g_\parallel = 2.236$, $g_\perp = 2.051$, $A_\parallel = 163$ G.

The ESR spectra of $[ZnMn(H_2L^1)Cl_2]$ **6** in dimethylformamide at room and liquid-nitrogen temperature are shown in Figs. 1 and 2, respectively. In the fluid a six-line hyperfine splitting of ^{55}Mn ($I = \frac{5}{2}$) is observed with $g_{iso} = 2.00$ and

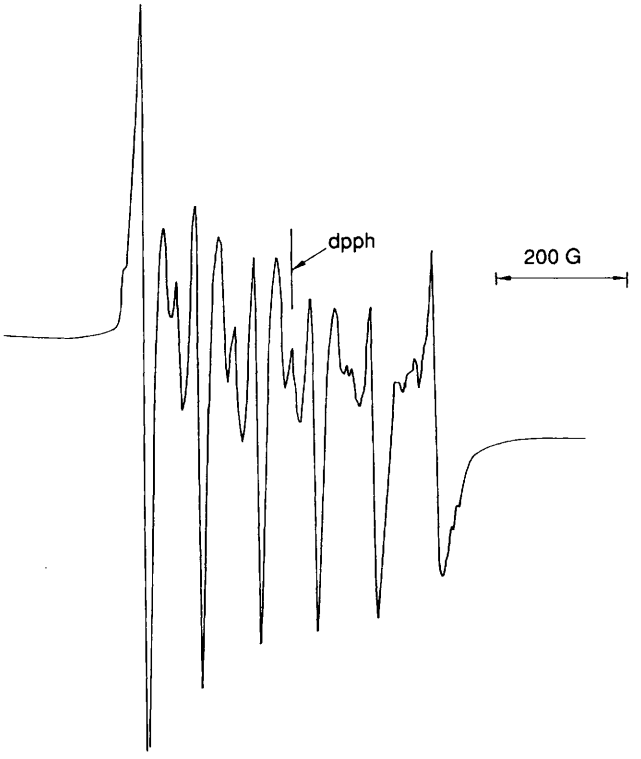

Fig. 2 The ESR spectrum of $[ZnMn(H_2L^1)Cl_2]$ **6** in dimethylformamide solution at 77 K. Microwave frequency 9.72 GHz

$A_{iso} = 90$ G. The frozen-glass spectrum shows a sixteen-line feature, which is similar to that reported for manganese(II) ion in polycrystalline and glassy material.[28,29] The spectrum actually shows six main lines, between each pairs of which there is a doublet. The intensity of the doublet decreases at higher fields. The six main lines are the hyperfine spectrum of manganese(II) ion ($S = \frac{5}{2}$) for the $-\frac{1}{2} \longrightarrow +\frac{1}{2}$ transition; the isotropic $g = 2.00$ and $A = 90$ G values conform to a $^6A_1$ ground state, which is well separated from the other energy states. In polycrystalline or glassy material the other fine structures due to $\pm\frac{5}{2} \longrightarrow \pm\frac{3}{2}$ and $\pm\frac{3}{2} \longrightarrow \pm\frac{1}{2}$ transitions are not observed as they are unresolvably broadened due to the anisotropic effect of the zero-field splitting.[29] The occurrence of the five doublets has been attributed[30,31] to forbidden $\Delta M = \pm 1$ transitions (M is the nuclear magnetic quantum number), which are brought about by mixing of the nuclear hyperfine levels by the zero-field splitting parameter.

Crystal structures

$[Fe_2(H_2L^1)_4(\mu\text{-}OH)_2]\cdot 4H_2O$ 7. A perspective view of the

Table 3 Crystal data[a] for $[Fe_2(H_2L^1)_4(\mu\text{-}OH)_2]\cdot 4H_2O$ **7** and $[Cu_2(H_2L^1)(acac)_2][ClO_4]\cdot CHCl_3$ **2**·$CHCl_3$

	7	**10**·$CHCl_3$
Formula	$C_{60}H_{70}Fe_2N_{16}O_{10}$	$C_{26}H_{30}Cl_4Cu_2N_4O_9$
M	1287.0	811.4
a/Å	14.482(5)	11.590(5)
b/Å	16.262(6)	12.374(4)
c/Å	16.530(6)	13.826(5)
α/°	117.53(2)	99.23(3)
β/°	98.96(2)	91.65(3)
γ/°	105.43(2)	94.23(3)
U/Å^3	3145.4	1950.2
D_c/g cm^{-3}	1.359	1.382
λ/Å	1.5418 (Cu-Kα)	0.710 73 (Mo-Kα)
Transmission ranges/%	99.8–46.9	84.0–62.1
Reflections measured	9216	9360
Reflections observed [$I > 3\sigma(I)$]	4844	8990
R^b	0.046	0.148
R'^c	0.025	

[a] Details in common: triclinic, space group $P\bar{1}$, $Z = 2$. [b] $R(F_o) = \Sigma||F_o| - |F_c||/\Sigma|F_o|$. [c] $R'(F_o) = (\Sigma w||F_o| - |F_c||^2/\Sigma w|F_o|^2)^{\frac{1}{2}}$. $w = 3F/F_{max}$ if $F < \frac{1}{3}F_{max}$; $F_{max}/3F$ if $F > \frac{1}{3}F_{max}$.

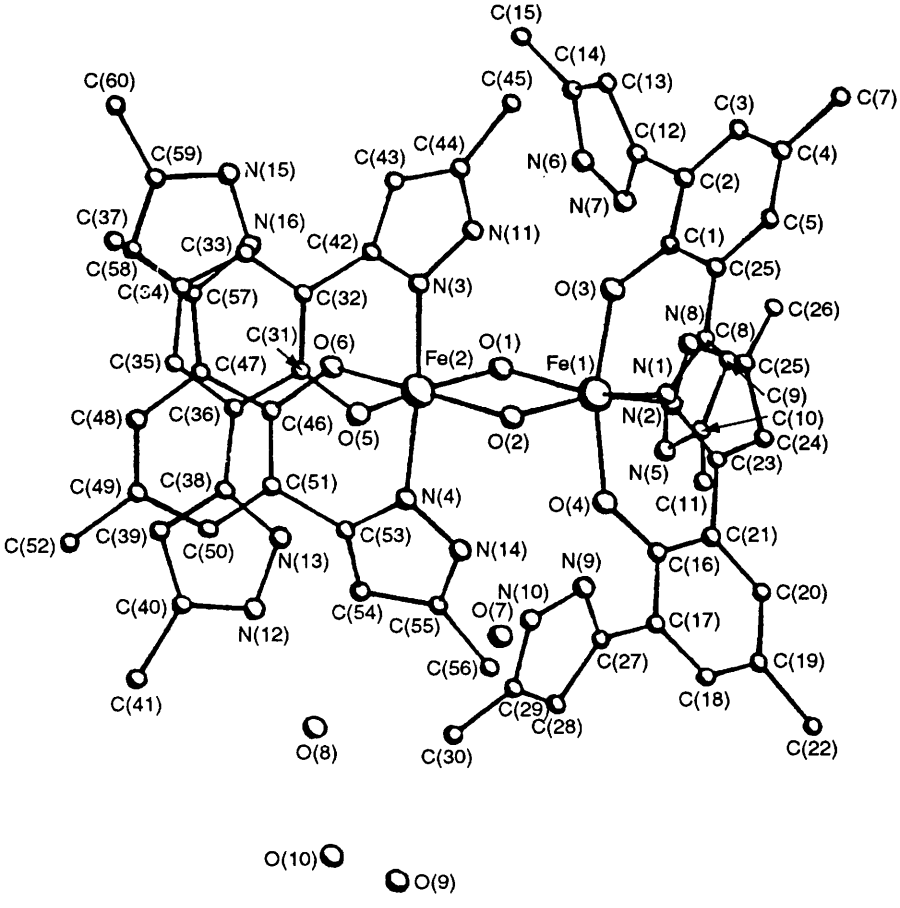

Fig. 3 Perspective view of the molecular structure of the diiron(III) complex $[Fe_2(H_2L^1)_4(\mu\text{-}OH)_2]\cdot 4H_2O$ **7**

molecular structure of complex **7** is shown in Fig. 3 along with the atom-labelling scheme. Bond distances and angles pertaining to the iron(III) co-ordination spheres are given in Table 4.

The structure comprises two FeO_2N_2 co-ordination cores linked by two hydroxyl groups, which leads to edge sharing between FeO_4N_2 octahedra. Unlike complexes **1**–**6**, in **7** the phenolate oxygen atom of the ligand is not involved in bridging the two metal centres. The H_3L^1 in this case acts as a bidentate ligand and utilizes one of the pyrazolyl nitrogen atoms and the phenolate oxygen atom for binding iron(III). The two metal centres, in turn, are stereochemically non-equivalent, that is the spatial configurations of the two FeO_4N_2 octahedra are different. For example, with Fe(1) the co-ordinated nitrogen atoms N(1) and N(2) are in equatorial positions and are *cis* with respect to each other, while the phenolate oxygen atoms O(3) and O(4) occupy the *trans* axial positions. On the other hand, with Fe(2) the situation is reversed, that is, N(3) and N(4) are in *trans* configuration whereas the phenolate oxygen atoms O(5) and O(6) occupy *cis* positions in the basal plane. A consideration of the metal planes reveals that the atoms N(1), N(2), O(1) and O(2) are alternately displaced above and

Table 4 Selected bond distances (Å) and angles (°) for $[Fe_2(H_2L^1)_4(\mu\text{-}OH)_2]\cdot 4H_2O$ **7**

Fe(1)–O(1)	2.031(2)	Fe(2)–O(1)	2.036(2)
Fe(1)–O(2)	2.017(2)	Fe(2)–O(2)	1.990(2)
Fe(1)–O(3)	1.915(2)	Fe(2)–O(5)	1.964(3)
Fe(1)–O(4)	1.929(4)	Fe(2)–O(6)	1.962(3)
Fe(1)–N(1)	2.114(2)	Fe(2)–N(3)	2.080(3)
Fe(1)–N(2)	2.132(2)	Fe(2)–N(4)	2.096(3)
Fe(1) · · · Fe(2)	3.174(4)		
O(1)–Fe(1)–O(2)	76.2(2)	O(1)–Fe(2)–O(2)	76.6(2)
N(1)–Fe(1)–N(2)	101.4(2)	O(5)–Fe(2)–O(6)	93.7(2)
O(1)–Fe(1)–O(3)	85.89(8)	O(1)–Fe(2)–N(3)	93.2(1)
O(1)–Fe(1)–O(4)	105.08(8)	O(1)–Fe(2)–N(4)	91.0(1)
O(2)–Fe(1)–O(3)	108.69(8)	O(2)–Fe(2)–N(4)	93.8(1)
O(2)–Fe(1)–O(4)	84.88(7)	O(2)–Fe(2)–N(3)	91.3(1)
N(1)–Fe(1)–O(3)	83.20(8)	O(5)–Fe(2)–N(3)	84.4(1)
N(1)–Fe(1)–O(4)	90.2(2)	O(5)–Fe(2)–N(4)	92.5(1)
N(2)–Fe(1)–O(3)	88.1(2)	O(6)–Fe(2)–N(3)	91.3(1)
N(2)–Fe(1)–O(4)	79.5(3)	O(6)–Fe(2)–N(4)	83.9(1)
N(1)–Fe(1)–O(2)	87.33(8)	O(2)–Fe(2)–O(5)	90.6(2)
N(2)–Fe(1)–O(1)	99.53(7)	O(1)–Fe(2)–O(6)	99.2(2)
N(1)–Fe(1)–O(1)	156.08(7)	O(1)–Fe(2)–O(5)	166.9(1)
N(2)–Fe(1)–O(2)	162.09(8)	O(2)–Fe(2)–O(6)	175.2(2)
O(3)–Fe(1)–O(4)	164.53(8)	N(3)–Fe(2)–N(4)	174.1(1)
Fe(1)–O(1)–Fe(2)	102.6(1)	Fe(2)–O(2)–Fe(1)	104.7(1)

below the best plane of Fe(1) by 0.218–0.329 Å. However, corresponding displacements of the atoms O(1), O(2), O(5) and O(6) from the least-squares plane of Fe(2) occur within a narrow range of 0.035–0.044 Å. The structural data (Table 4) clearly indicate that the Fe(2) centre has a relatively more regular octahedral geometry. The dihedral angle between the planes of these two metal centres is 12.7(2)°.

The bond distances and angles given in Table 4 indicate distorted-octahedral geometries of the iron centres. It may be noted that the axial Fe–O(phenolate) distances [Fe(1)–O(3) 1.915(2), Fe(1)–O(4) 1.929(4) Å] are shorter relative to the equatorial Fe–O(phenolate) distances [Fe(2)–O(5) 1.964(3), Fe(2)–O(6) 1.962(3) Å]. Further, the Fe–O(phenolate) distances are relatively shorter compared to the Fe–O(hydroxy) distances. Again, the in-plane Fe–N bonds [Fe(1)–N(1) 2.114(2), Fe(1)–N(2) 2.132(2) Å] are longer compared to the axial Fe–N bonds [Fe(2)–N(3) 2.080(3), Fe(2)–N(4) 2.096(3) Å]. In general, all the *cis* and *trans* angles deviate more or less from 90 and 180°, especially the *transoid* linkage O(3)–Fe(1)–O(4) is appreciably kinked, 164.5(1)°. The four-membered $Fe_2(\mu\text{-}OH)_2$ ring forms an exact plane in which the two metal centres are held apart by 3.17 Å with two slightly different Fe–OH–Fe bridge angles of 102.6(1) and 104.7(1)°.

$[Cu_2(H_2L^1)(acac)_2][ClO_4]\cdot CHCl_3$ 2·$CHCl_3$. As already mentioned, due to significant crystal decay and disorder the refinement of the structure did not reach a satisfactory level. Nevertheless, the cation seems to have been determined well and a perspective view is shown in Fig. 4. The metrical parameters of the copper co-ordination spheres indicated almost regular square-planar geometries for both. Indeed, all the Cu–O and Cu–N distances are quite similar [average 1.91(2) Å] and there is a small deviation of *cis*-angles from 90 (± 4)°. The two copper(II) centres are supported by a single phenoxide bridge with a Cu–O–Cu angle of 103.5° and the non-bonding Cu · · · Cu distance is 3.03 Å.

Electrochemistry

Cyclic voltammetric studies have been carried out for the homodinuclear complexes $[Cu_2(H_2L^1)_2][ClO_4]_2$ **1**, $[Cu_2(H_2L^1)(\mu\text{-}OH)Cl_2]$ **3**, $[Ni_2(H_2L^1)_2(H_2O)_4][ClO_4]_2$ **4** and $[Fe_2(H_2L^1)_4(\mu\text{-}OH)_2]\cdot 4H_2O$ **7**. In Me_2SO, reduction of the dicopper(II) complexes **1** and **3** take place irreversibly at −0.65 and −0.50 V *vs.* Ag–AgCl, respectively. Similar irreversible reduction of the dinickel(II) complex **4** takes place at −1.10 V. However, unlike **1** and **3**, which are resistant to oxidation in MeCN solutions up to 1.6 V, **4** undergoes irreversible oxidation at 1.05 V. The diiron(III) complex **7** experiences stepwise reductions, albeit irreversibly, in MeCN at −0.12 and −0.70 V.

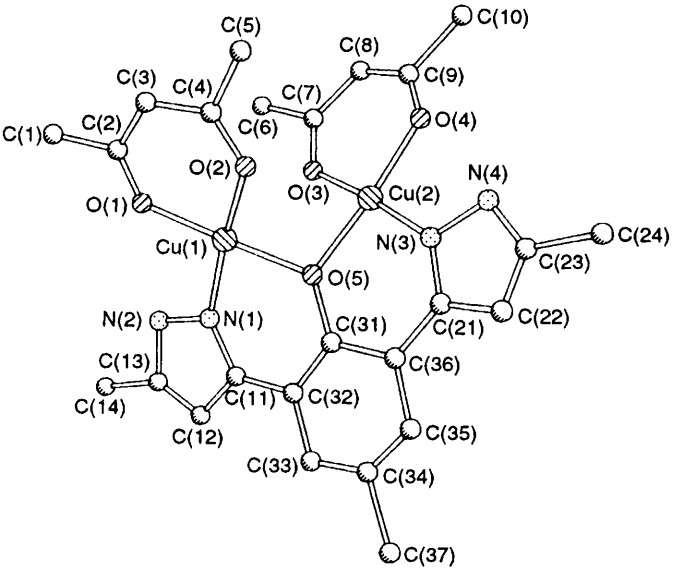

Fig. 4 Perspective view of the $[Cu_2(H_2L^1)(acac)_2]^+$ cation in complex **2**·$CHCl_3$

Magnetic properties

Variable-temperature (80–295 K) magnetic susceptibility data were collected for the dicopper(II) complexes **1**–**3**, dinickel(II) complex **4** and diiron(III) complexes **7**–**9**. Plots of χ_m *vs.* T for some of these compounds are illustrated in Figs. 5–7. The susceptibility data for the homodinuclear systems were fitted by the theoretical expressions (2)–(4) obtained by considering

$$S_1 = S_2 = \tfrac{1}{2}$$

$$\chi_m = C(1-p)\cdot\frac{2e^{2x}}{1+3e^{2x}} + \tfrac{1}{4}Cp + \text{t.i.p.} \qquad (2)$$

$$S_1 = S_2 = 1$$

$$\chi_m = C(1-p)\cdot\frac{2e^{2x}+10e^{6x}}{1+3e^{2x}+5e^{6x}} + \tfrac{2}{3}Cp + \text{t.i.p.} \qquad (3)$$

$$S_1 = S_2 = \tfrac{5}{2}$$

$$\chi_m = C(1-p)\cdot\frac{2e^{2x}+10e^{6x}+28e^{12x}+60e^{20x}+110e^{30x}}{1+3e^{2x}+5e^{6x}+7e^{12x}+9e^{20x}+11e^{30x}} + 4.4\frac{2p}{T} + \text{t.i.p.} \qquad (4)$$

isotropic exchange interaction between two spin centres $S_1 = S_2 = \frac{1}{2}(Cu^{2+})$, $1(Ni^{2+})$ or $\frac{5}{2}(Fe^{3+})$ as governed by the spin Hamiltonian $\mathcal{H} = -2JS_1\cdot S_2$. The symbols N, β, g and k in these expressions have their usual meanings, p represents the fraction of mononuclear paramagnetic impurity present, $C = N\beta^2g^2/kT$ and $x = J/kT$. The temperature-independent paramagnetic susceptibility (t.i.p.) was considered to be 120×10^{-6} cm^3 mol^{-1} for **1**–**3**, 200×10^{-6} cm^3 mol^{-1} for **4** and 160×10^{-6} cm^3 mol^{-1} for **7**–**9**.

The best-fit lines shown in Figs. 5–7 were obtained by non-linear regression analysis and the results are given in Table 5. The shapes of these plots are clearly indicative of antiferromagnetic exchange interactions in all the compounds. Antiferromagnetic behaviour of the dinickel(II) complex **4** was also evident from the fact that the effective magnetic moment

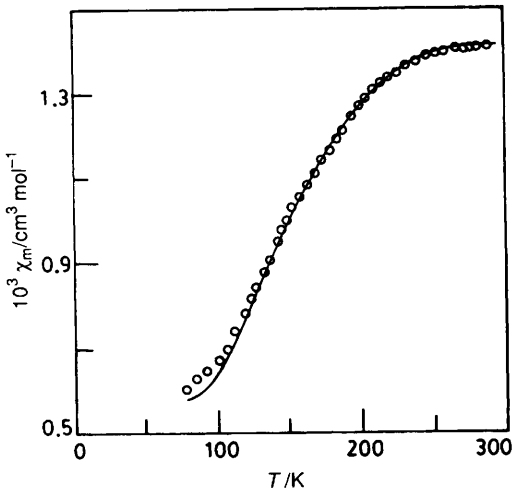

Fig. 5 Molar susceptibility (χ_m) *vs.* temperature (T) for $[Cu_2(H_2L^1)(acac)_2][ClO_4]$ **2**. The solid line results from a least-squares fit by the theoretical equation (2) given in the text

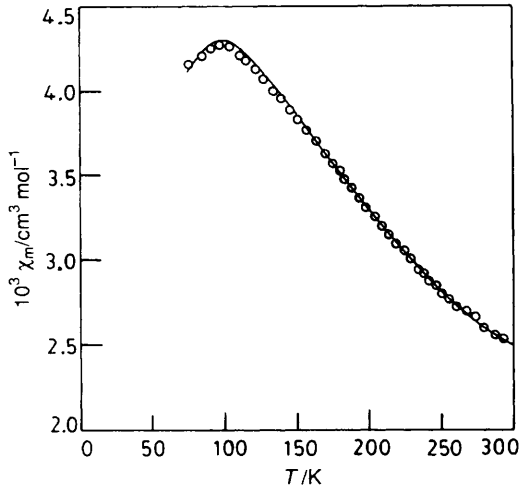

Fig. 6 Molar susceptibility *vs.* temperature for $[Cu_2(H_2L^1)(\mu\text{-}OH)Cl_2]$ **3**. The solid line results from a least-squares fit by the theoretical equation (2)

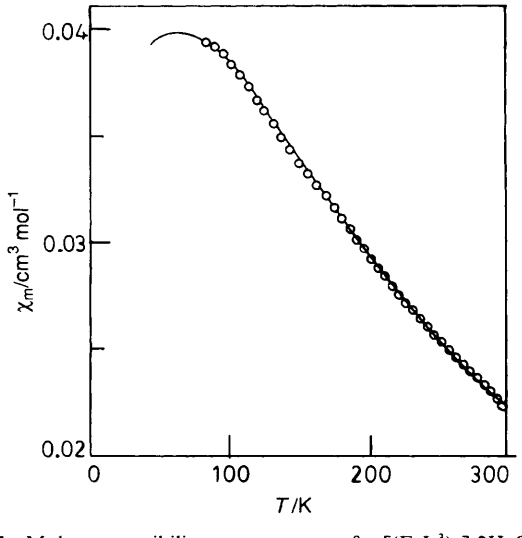

Fig. 7 Molar susceptibility *vs.* temperature for $[(FeL^3)_2]\cdot 2H_2O$ **9**. The solid line results from a least-squares fit by the theoretical equation (4)

per nickel(II) decreases monotonically from 3.00 μ_B at 295 K to 2.68 μ_B at 81 K.

The results given in Table 5 show that for the dicopper(II) complexes the values of the singlet–triplet energy difference

Table 5 Magnetic data for the complexes

Complex	J/cm^{-1}	g	p (%)
1	−242	2.11	4
2	−55	2.10	0.2
3	−170	2.08	3
4	−24	2.16	1
7	−11.0	2.00	5
8	−15.7	2.00	0.5
9	−8.8	2.00	0

($-2J$) decrease in the following way: **1** (484) > **3** (340) > **2** (110 cm^{-1}). Complexes **1**–**3** differ in the nature of the bridging between the copper centres. Thus, while in **1** there are two equivalent phenoxide bridges, in **3** the two bridging units (phenoxide and hydroxide) are non-equivalent; on the other hand, the two metal centres in **2** are supported by a single phenoxide bridge. The minimum value of $-2J$ observed for **2** indicates that the superexchange involving $d_{x^2-y^2}$–(s, p_x, p_y)–$d_{x^2-y^2}$ orbitals is less efficacious when the pathway involves a single bridge. The greater value of $-2J$ observed for **1** relative to that of **3** can be related to two factors. First, it is now known [32] that for a given Cu–O–Cu bridge angle (> 97.5°) the singlet–triplet energy gap is greater in a diphenoxo- than a dihydroxo-bridged compound. Secondly, in $[Cu_2(H_2L^1)(\mu\text{-}OH)Cl_2]$ **3** depletion of electron density occurs for the magnetic orbital $d_{x^2-y^2}$ of copper(II) due to the co-ordinated chlorine atom, and as a consequence the magnitude of the spin-exchange integral is reduced. In an earlier study we have shown [33] that in a series of isostructural diphenoxo-bridged dicopper(II) complexes $[Cu_2(L^2)X_2]$ (X = Cl, Br or I) the values of $-2J$ decrease monotonically with the increase in electron affinity of the halogens.

The dinickel(II) complex **4** exhibits antiferromagnetic behaviour with an exchange coupling constant ($-J$) of 24 cm^{-1}. We have recently demonstrated [34] for a series of phenoxo-bridged dinickel(II) complexes with centrosymmetric structures that the exchange coupling constants bear a linear relationship with the corresponding Ni–O–Ni bridge angles. More recently Staemmler and co-workers [35] have provided a theoretical foundation to this observation. We note that **4** is most likely to have a centrosymmetric structure and its Ni–O–Ni bridge angle(s) is predicted to be *ca.* 101°.

All the three diiron(III) complexes **7**–**9** are weakly antiferromagnetic, the $-J$ values decreasing the order **8** (15.7) > **7** (11.0) > **9** (8.8 cm^{-1}). For doubly- and triply-bridged dinuclear iron(III) complexes Gorun and Lippard [36] have proposed a magnetostructural relationship (5), which

$$-J = 8.763 \times 10^{11} \exp(-12.663P) \qquad (5)$$

correlates the antiferromagnetic coupling constant with a structural parameter P, describing the shortest superexchange pathway between the two metal centres. In the case of **7** the shortest distance between the iron and bridging oxygen atoms is 1.990 Å (Table 4). Using this as the value of P one obtains $-J$ = 9.9 cm^{-1}, which agrees reasonably with the observed value of $-11.0\ cm^{-1}$.

Complexes **8** and **9** are likely to have similar structures in which the central phenolate oxygen atom is bridging the two iron centres (as illustrated for **9**). However, **9** is expected to have a more flexible configuration because it is derived from a ligand in which the phenyl rings are connected by strain-free CH_2NHCH_2 linkages. It is reasonable to expect that the Fe–O distances in the $Fe(\mu\text{-}O)_2Fe$ ring will be greater in the case of **9** than in **8** due to its less-strained configuration. In other words, the value of P will be less for **8**. It follows from equation (5) that with the decrease of P the magnitude of $-J$ will increase.

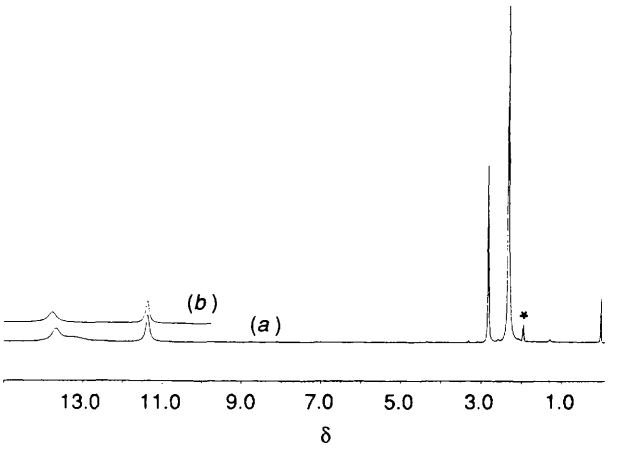

Fig. 8 Proton NMR spectra of $[Cu_2(H_2L^1)_2][ClO_4]_2$ **1** at room temperature in (*a*) CD_3CN solution and (*b*) CD_3CN–D_2O solution. The asterisk indicates the solvent peak

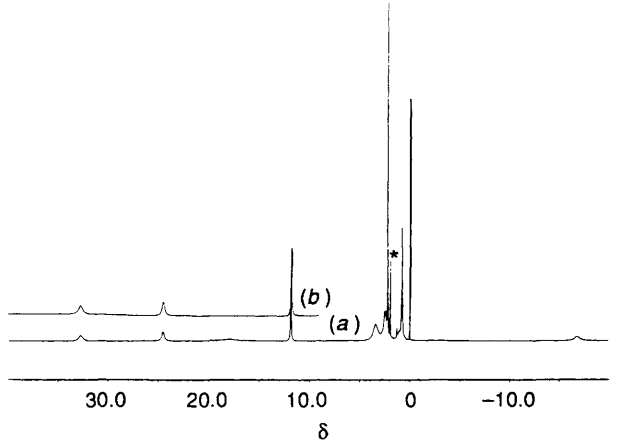

Fig. 9 Proton NMR spectra of $[Cu_2(H_2L^1)(acac)_2][ClO_4]$ **2**. Details as in Fig. 8

This is in accord with the observed antiferromagnetic coupling constants of **8** (−15.7) and **9** (−8.8 cm^{-1}).

Proton NMR spectroscopy

For paramagnetic copper(II) complexes generally, broadening of proton NMR resonances occurs to a significant extent due to slow electronic relaxation.[37] However, recent studies with several antiferromagnetically coupled dicopper(II) complexes have produced reasonably sharp high-resolution spectra.[38] It has been suggested[38] that the narrowing of linewidths in these systems is governed by multiple relaxation mechanisms.

The ^1H NMR spectra of $[Cu_2(H_2L^1)_2][ClO_4]_2$ **1** and $[Cu_2(H_2L^1)(acac)_2][ClO_4]$ **2** in CD_3CN–D_2O (also in neat CD_3CN) at room temperature are shown in Figs. 8 and 9, respectively. For both compounds reasonably sharp well resolved signals are observed. However, as may be noted while for **1**, the chemical shifts occur over a relatively small range, δ 2–14, δ 18 to 34 for **2**. Clearly, the range is controlled by the strength of the antiferromagnetic coupling between the two copper centres, which is consistent with the notion that the contact shift of a particular ligand proton is proportional to the magnetic susceptibility of the complex.[5]

The remarkably simple spectrum of complex **1** (Fig. 8) is due to its symmetric structure in solution. A broad feature observed at *ca.* δ 13 in CD_3CN solution which disappears on addition of D_2O is attributable to the pyrazolyl protons. The assignment of the other resonances has been made by considering relative peak areas and their proximity to the metal centres. Thus, the two sharp signals at δ 2.25 and 2.75 are due to *p*-CH_3 and pyrazolyl CH_3 resonances, while the two broader peaks at δ 11.4 and 13.8 can be assigned to the aromatic and pyrazole ring protons, respectively.

The absence of a two-fold axis of symmetry noted in the solid-state structure of complex **2** is also evident in its ^1H NMR spectrum (Fig. 9). Four different methyl resonances are observed at δ 0.8, 2.6, 2.9 and 3.4. The aromatic protons are shifted to δ 11.8 and the resonance at δ 18 is subject to exchange upon addition of D_2O. We tentatively assign the peaks at δ 24.5 and 33 to pyrazole ring protons and that at δ −17 to the π-delocalized acetylacetonate ring protons.

To conclude, we note that $[Cu_2(H_2L^1)(acac)_2][ClO_4]$ provides a rare example of a dinuclear heterochelate. Preliminary studies indicate that the dicopper(II) and dinickel(II) complexes can be deprotonated (pyrazolyl NH) and then induced to bind additional metal ions using auxiliary ligands. Further, it is possible to synthesize neutral tris(chelates) $M(N,O^-)_3$ of H_3L^1 and to use them as building blocks for polynuclear assemblies. Work in these directions is in progress.

Acknowledgements

This research was supported by the Science and Engineering Research Council of the Department of Science and Technology, Government of India. We thank Dr. P. Chaudhuri of the Ruhr University, Bochum for variable-temperature magnetic measurements. Preliminary X-ray crystallographic measurements made for the iron complex by the late Dr. K. Venkatsubramanian are gratefully acknowledged.

References

1 O. Kahn, *Molecular Magnetism*, VCH, New York, 1993.
2 *Magnetic Molecular Materials*, eds. D. Gatteschi, O. Kahn, J. S. Miller and F. Palacio, Kluwer Academic, Dordrecht, 1990.
3 P. Zanello, S. Tamburini, P. A. Vigato and G. A. Mazzochin, *Coord. Chem. Rev.*, 1987, **77**, 165.
4 A. Bencini and D. Gatteschi, *EPR of Exchange Coupled Systems*, Springer, Berlin, 1990.
5 I. Bertini and C. Luchinat, *NMR of Paramagnetic Molecules in Biological Systems*, Benjamin-Cummings, Boston, 1986.
6 P. A. Vigato, S. Tamburini and D. E. Fenton, *Coord. Chem. Rev.*, 1990, **106**, 205.
7 *Metal Clusters in Proteins*, ed. L. Que, jun., American Chemical Society, Washington, DC, 1988.
8 W. E. Hatfield, in *Theory and Applications of Molecular Paramagnetism*, eds. E. S. Bordeaux and L. N. Mulay, Wiley, New York, 1976, p. 350.
9 A. P. Ginsberg, *Inorg. Chim. Acta Rev.*, 1971, **5**, 45.
10 D. Gatteschi, A. Caneschi, L. Pardi and R. Sessoli, *Science*, 1994, **265**, 1045 and refs. therein.
11 T. S. Sorrell, *Tetrahedron*, 1989, **45**, 1.
12 K. D. Karlin and Y. Gultneh, *Prog. Inorg. Chem.*, 1987, **35**, 219.
13 L. Que, jun. and A. E. True, *Prog. Inorg. Chem.*, 1990, **38**, 97.
14 N. H. Pilkington and R. Robson, *Aust. J. Chem.*, 1970, **23**, 2225; A. J. Edwards, B. F. Hoskins, E. H. Kachab, A. Markiewicz, K. S. Murray and R. Robson, *Inorg. Chem.*, 1992, **31**, 3585.
15 H. Okawa, M. Tadokoro, Y. Aratake, M. Ohba, K. Shindo, M. Mitsumi, M. Koirawa, M. Tomono and D. E. Fenton, *J. Chem. Soc., Dalton Trans.*, 1993, 253; H. Okawa, J. Nishio, M. Ohba, M. Tadokoro, M. Matsumoto, M. Koikawa, S. Kida and D. E. Fenton, *Inorg. Chem.*, 1993, **32**, 2949.
16 K. K. Nanda, K. Venkatsubramanian, D. Majumdar and K. Nag, *Inorg. Chem.*, 1994, **33**, 1581; K. K. Nanda, S. K. Dutta, S. Baitalik, K. Venkatsubramanian and K. Nag, *J. Chem. Soc., Dalton Trans.*, 1995, 1239 and refs. therein.
17 V. McKee and S. S. Tandon, *J. Chem. Soc., Dalton Trans.*, 1991, 221.
18 A. J. Atkins, A. J. Blake and M. Schroder, *J. Chem. Soc., Chem. Commun.*, 1993, 353; 1662.
19 P. J. Steel, *Coord. Chem. Rev.*, 1990, **106**, 227.
20 S. K. Mandal and K. Nag, *J. Chem. Soc., Dalton Trans.*, 1983, **22**, 2567.
21 N. A. Bailey, D. E. Fenton, J. Lay, P. B. Roberts, J.-M. Latour and D. Limosin, *J. Chem. Soc., Dalton Trans.*, 1986, 2681.

22 M. Bell, A. J. Edwards, B. F. Hoskins, E. H. Kachab and R. Robson, *J. Am. Chem. Soc.*, 1989, **111**, 3603.
23 A. C. T. North, D. C. Phillips and F. S. Mathews, *Acta Crystallogr., Sect. A*, 1968, **24**, 351.
24 P. Main, G. Germain, J. P. Declercq and M. M. Woolfson, MULTAN 82, A System of Computer Programs for the Automatic Solution of Crystal Structures from X-Ray Data, University of York, 1982.
25 G. M. Sheldrick, SHELXTL PLUS Program Package (PC Version), University of Göttingen, 1989.
26 G. M. Sheldrick, SHELXL 93, A Program for Crystal Structure Refinement, Gamma-Test Version, University of Göttingen, 1993.
27 D. T. Cromer and J. T. Waber, *International Tables for X-Ray Crystallography*, Kynoch Press, Birmingham, 1974, vol. 4.
28 B. T. Allen and D. W. Nebert, *J. Chem. Phys.*, 1964, **41**, 1983.
29 B. T. Allen, *J. Chem. Phys.*, 1965, **43**, 3820.
30 B. Bleaney and R. S. Rubins, *Proc. Phys. Soc.*, 1961, **77**, 103.
31 E. Friedman and W. Low, *Phys. Rev.*, 1960, **120**, 408.
32 K. Nag, *Proc. Indian Acad. Sci.* (*Chem. Sci.*), 1990, **102**, 269 and refs. therein.
33 S. K. Mandal, L. K. Thompson, M. J. Newlands, E. J. Gabes and K. Nag, *Inorg. Chem.*, 1990, **29**, 1324.
34 K. K. Nanda, L. K. Thompson, J. N. Bridson and K. Nag, *J. Chem. Soc., Chem. Commun.*, 1994, 1337; K. K. Nanda, R. Das, L. K. Thompson, K. Venkatsubramanian, P. Paul and K. Nag, *Inorg. Chem.*, 1994, **33**, 1188.
35 C. Wang, K. Fink and V. Staemmler, *Chem. Phys.*, 1995, **192**, 25.
36 S. M. Gorun and S. J. Lippard, *Inorg. Chem.*, 1991, **30**, 1625.
37 I. Bertini, P. Turano and A. J. Vila, *Chem. Rev.*, 1993, **93**, 2833.
38 J. H. Satcher, jun., and A. L. Balch, *Inorg. Chem.*, 1995, **34**, 3371.

Received 18*th December* 1995; *Paper* 5/08199H